Rib Cartilage Characterization in Patients Affected by Pectus Excavatum

FRANCESCA TOCCHIONI,[1] MARCO GHIONZOLI,[1]* LAURA CALOSI,[2] DANIELE GUASTI,[2] PAOLO ROMAGNOLI,[2] AND ANTONIO MESSINEO[1]

[1]Department of Pediatric Surgery, University of Florence and Children's University Hospital A. Meyer, Florence, Italy

[2]Department of Experimental and Clinical Medicine, University of Florence, Italy

ABSTRACT

Pectus excavatum (PE) is the most frequent anterior chest deformity which may be frequently associated with connective tissue disorders. We performed microscopic analyses to better understand cartilage behavior and obtain clues on its pathogenesis. In 37 PE patients, none with Marfan syndrome, we analyzed costal cartilage by light microscopy, immunohistochemistry and transmission electron microscopy. Control tissue specimens were harvested from four patients without any connective tissue disease. In both control and PE patients, chondrocytes were on the average <15 μm in diameter and occupied $<10\%$ of tissue volume; in most cases the extracellular matrix was stained by alcian blue, instead of safranin; no difference between PE and control samples was significant. All samples showed an uneven collagen type II immunolabeling both within the cells and pericellular matrix, and occasionally of the territorial matrix. In all cases numerous cells underwent apoptosis accompanied by matrix condensation as shown by electron microscopy. Our results suggest that matrix composition and the cell number and size of costal cartilage are dependent on the subject and not on the disease; the microscopic organization of cartilage is correlated with the stabilization of the defective shape rather than with the onset of the deformity. Anat Rec, 00:000–000, 2013.

Key words: pectus excavatum; rib cartilage; marfan; fibrillin; fibrillinopathies

Pectus excavatum (PE) is characterized by prominent depression of the sternum and adjacent costal cartilages, generally extending from the third to seventh rib. It accounts for ~90% of the congenital deformities of the chest wall and has been estimated to have an incidence of 1 in 300 to 1 in 1,000 live births, with a male/female ratio of ~4:1 (Cartoski et al., 2006; Tocchioni et al., 2012).

The chest wall depression usually becomes evident within the first year of life and increases in severity during pubertal spurt (Jaroszewski et al., 2010; Brochhausen et al., 2012). It is associated with a characteristic morphology: the patients are thin, tall, with abdominal protrusion and shoulders which are bent forward, a typical posture which may lead to or aggravate scoliosis. Dyspnea, fatigue, chest pain and palpitations may be present in some patients (Brochhausen et al., 2012). About 40% patients with PE have family members affected by various skeletal deformities: PE, other sternal defects (Jaroszewski et al., 2010; Tocchioni et al., 2012). PE is frequently associated with heritable connective tissue diseases, especially Marfan syndrome (MFS) or MASS phenotype (mitral valve prolapse, not-progressive aortic enlargement, skeletal and skin alterations), which it is present in about 70% of PE cases

*Correspondence to: Marco Ghionzoli, MD, PhD, Department of Pediatric Surgery, University of Florence and Children's University Hospital A. Meyer, Florence, Italy. Fax: +39-055-5662400. E-mail: m.ghionzoli@meyer.it

Received 29 May 2013; Accepted 25 September 2013.

DOI 10.1002/ar.22824

Published online 00 Month 2013 in Wiley Online Library (wileyonlinelibrary.com).

(Golladay et al., 1985; Scherer et al., 1988; Glesby and Pyeritz, 1989; Redlinger et al., 2010; Tocchioni et al., 2012). MFS is an autosomal dominant connective tissue disease caused by mutations in the gene *FBN1* encoding the glycoprotein fibrillin-1, which is a component of elastic and oxytalan fibers. The incidence of MFS is two to three cases in 10,000 live birth (Olbrecht et al., 2009; Redlinger et al., 2010). MFS is multisystemic and clinical manifestations vary in range and severity (Dietz, 1992; Nollen and Mulder, 2004): cardiovascular involvement (aortic dilatation and dissection) are the major cause of morbidity and mortality (Judge and Dietz, 2005; Stuart and Williams, 2007). MASS is an autosomal dominant disease which is also caused by mutations in the *FBN1* gene (Le Parc et al., 2000; Chaffins, 2007; Mortensen et al., 2010). It belongs to connective tissue disorders and is characterized by slight, generalized tissue laxity. Patients with MASS phenotype may have an aortic root diameter at the upper limits of normal, but progression to aneurysm or predisposition to dissection have never been documented (Glesby and Pyeritz, 1989; Dietz, 1992; Le Parc et al., 2000; Judge and Dietz, 2005; Loeys et al., 2010). These patients do not suffer from ectopia lentis (Dietz, 1992; Le Parc et al., 2000; Loeys et al., 2010) but appear to be prone to PE (Tocchioni et al., 2012).

We could find no information in the literature on the features of cartilage in MASS patients. Information is poor also regarding Marfan syndrome, although it has been reported that these patients are prone to growth cartilage deformation (Van de Velde et al., 2005) and to chondromalacia affecting hyaline cartilage (Shimode et al., 2007) besides elastic one (Fenton and Fagan, 1996). For Marfan syndrome, increase in lipid, glycogen and intermediate filaments of chondrocytes and amianthoid (asbestoid) degeneration of the matrix have been described in one report for which only the abstract was available to reading (Bardakhch'ian et al., 2002), or alternatively chondrocyte vacuolization and a decreased content in glycosaminoglycans and the presence of occasional wide collagen fibrils (Nogami et al., 1979).

The pathogenesis of PE is still uncertain. Many hypotheses have been put forward, such as intrauterine compression, rickets, pulmonary restriction, diaphragm alterations resulting in backward traction on the sternum, overgrowth of costal cartilage, and primary failure of osteogenesis or chondrogenesis (Creswick et al., 2006; Jaroszewski et al., 2010; Tocchioni et al., 2012).

A few studies have focused on histological, biochemical, biomechanical, genetics, and immunohistochemical analysis of costal cartilage of PE patients and all have yet failed to explain the pathogenesis of PE (Rupprecht et al., 1987; Feng et al., 2001; Creswick et al., 2006; Fokin et al., 2009; David et al., 2011; Stacey et al., 2012).

The aim of this study was to improve knowledge on tissue ultrastructural and biochemical features in PE patients and correlate them, whether possible, with the clinical phenotype, with the ultimate goal of better understanding the pathogenesis of the disease and achieving information of possible prognostic value to the large cohort of patients affected by PE and various collagen disorders.

METHODS

Thirty-seven consecutive patients affected by PE, of whom eight female, aged between 12 and 20 years, none with concurrent MFS, were operated at our institution from June 2011 to July 2012 with a minimally invasive technique (Nuss, 1998). Before the operation, every patient underwent chest nuclear magnetic resonance scan, electrocardiography, echocardiography, respiratory function evaluation. Moreover, we sought any clinical sign of connectivopathy according to a validated score (Glesby et al., 1989; Tocchioni et al., 2012) (Table 1). In strict agreement with Institutional Review Board approval we collected at surgery costal cartilage and skin samples from PE and one control patient without chest deformity who underwent a thoracic surgical procedure in the same time frame; three further control samples suitable for just light microscopy were obtained from archival biopsies of the University Pathology Department. Part of each specimen from patients and from the recently operated control was fixed in phosphate-buffered, 10% formalin, pH 7.4, for light microscopy, part was fixed in phosphate buffered 2% (w/v) formaldehyde and 2.5% (w/v) glutaraldehyde for electron microscopy.

TABLE 1. Diagnostic criteria for the MASS phenotype (each one: + = 1; − = 0)

• Mitral valve prolapse
• Nonspecific skeletal alterations (pectus excavatum, long limbs)
• Nonspecific skin alterations (striae atrophicae)
• Myopia (without ectopia lentis)

The further criterion of borderline and nonprogressive aortic enlargement was not used since all patients were below 21 years of age.

Light Microscopy

For light microscopic and histochemical analyses the specimens were dehydrated in ethanol and embedded in paraplast. Sections about 6-μm thick were deparaffinized and rehydrated. Cartilage sections were stained with hematoxylin-eosin, alcian blue pH 2.5-safranin pH 1, or with an indirect immunoperoxidase method for collagen II upon antigen retrieval (see below for details). For alcian blue-safranin staining the sections were rinsed in 3% acetic acid, stained 30 min with 1% (w/v) alcian blue (Bio-Optica, Milan, Italy) in 3% acetic acid, rinsed again in 3% HCl, stained 5 min with 0.3% (w/v) safranin O (Bio-Optica) in 0.125 mol L^{-1} HCl and rinsed in distilled water. This technique allows for an—albeit approximate—estimate of the distribution of highly sulfated glycosaminoglycans (safranine stained) and medium-to-not sulfated glycosaminoglycans (alcian blue stained). All stained sections were dehydrated, cleared and mounted in synthetic medium (Eukitt®, Fluka Sigma–Aldrich, Steinheim, Germany).

Morphometry

The relative volume of cells in the tissue was estimated from digitized photomicrographs of hematoxylin-eosin stained sections, taken with a 10× objective in a Leitz (Wetzlar, Germany) microscope equipped with a ProgRes C10plus camera (Jenoptik, Jena, Germany), by point counting with a square lattice test system with 500 points per mm^2 of tissue at final magnification 36,000×. The cell diameter was estimated from the

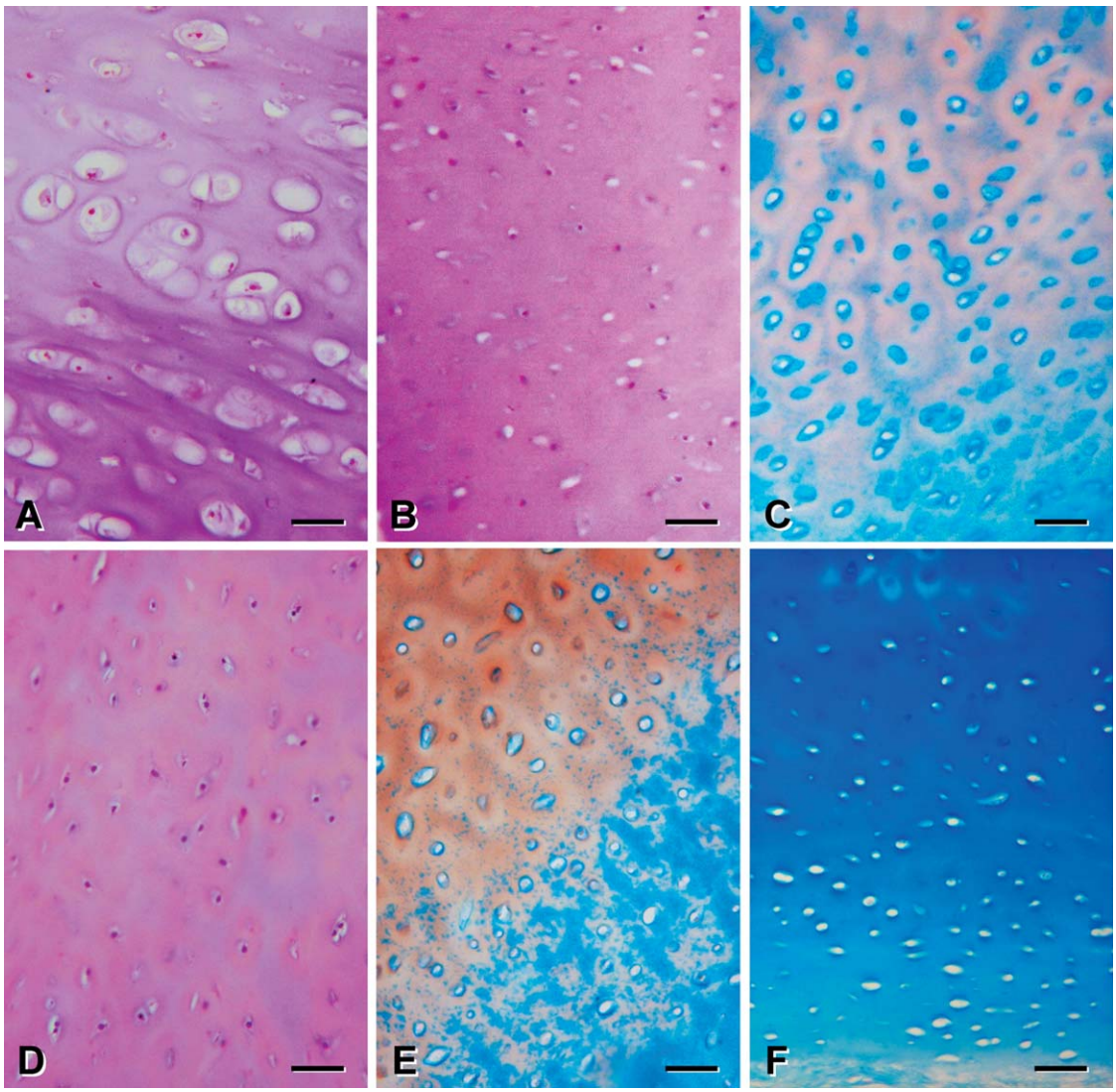

Fig. 1. Light microscopy of control and pectus excavatum cartilage. **A–C**: control cartilage. (A) Control cartilage from an archival biopsy of a 6-year-old child. Hematoxylin and eosin. (B) Cartilage of a subject 11-years old without PE: note much smaller and less frequent cells, single or in very small isogenic groups. Hematoxylin and eosin. (C) Cartilage of the same subject as B: alcian blue stain predominates close to the perichondrium, which was just below the bottom right end of microscopic field, safranin staining predominates deep in cartilage, where one recognizes alcian blue stained cell capsules surrounded by safranin stained haloes and mixed staining appears far from cells. Alcian blue and safranin. **D–F**: cartilage from pectus excavatum patients. (D) Cartilage of a patient 15-years old. Hematoxylin and eosin. (E) Cartilage of a patient 13-years old, which looks similar to the control depicted in C; the perichondrium was just below the bottom right end of microscopic field. Alcian blue and safranin. (F) Cartilage of a patient 12-years old, stained with alcian blue from the perichondrium (bottom of panel) to deep in cartilage (top of panel). Alcian blue and safranin. Bar = 5 μm.

same sections, upon thresholding to delineate the cell profile and measuring the cell section area with Image J (v 1.42; NIH, Bethesda, MD), at final magnification 33.65 nm/pixel; the diameter was computed from $D = 2(A/\pi)^{1/2}$. The relative volume of alcianophilic and respectively safraninophilic extracellular matrix was measured on digitized photomicrographs of alcian blue-safranine stained sections, as follows: the red stain was transformed into white with Photoshop (Adobe Systems, San Jose, CA), then the color was transformed into gray levels followed by thresholding and the surface area of black and white zones were measured with Image J (NIH), at final magnification 33.65 nm/pixel.

Immunohistochemistry

For antigen retrieval and collagen type II immunostaining the following steps were followed: removal of paraffin and hydration; citrate buffer 0.1 mol L^{-1}, pH 5.6, 15 min at 95°C in a water bath; cooling for 25 min and rinsing in distilled water; hydrogen peroxide 5 min, followed by rinsing in distilled water; 1.5% (w/v) serum albumin (Sigma, Milan, Italy) in 0.1 mol L^{-1} phosphate buffer, pH 7.4 (PBS), with 0.5% (v/v) Triton X-100 (Triton-PBS), 30 min at room temperature; anti-Col2 antibody (Abcam, Cambridge, UK; ab 3092, lot #GR83080-1), 1:100 in Triton-PBS, overnight at 4°C, followed by

TABLE 2. Quantitative analysis of cartilage cells and matrix (mean ± standard deviation)

	Cell diameter (μm)	Relative volume of cells	Relative volume of alcianophilic matrix (%)	*N*
Controls	43.25 ± 21.11	9.25 ± 4.19	68.67 ± 23.42	4
Pectus excavatum	35.71 ± 15.32	6.65 ± 2.83	58.07 ± 26.77	17

P not significant for all parameters.

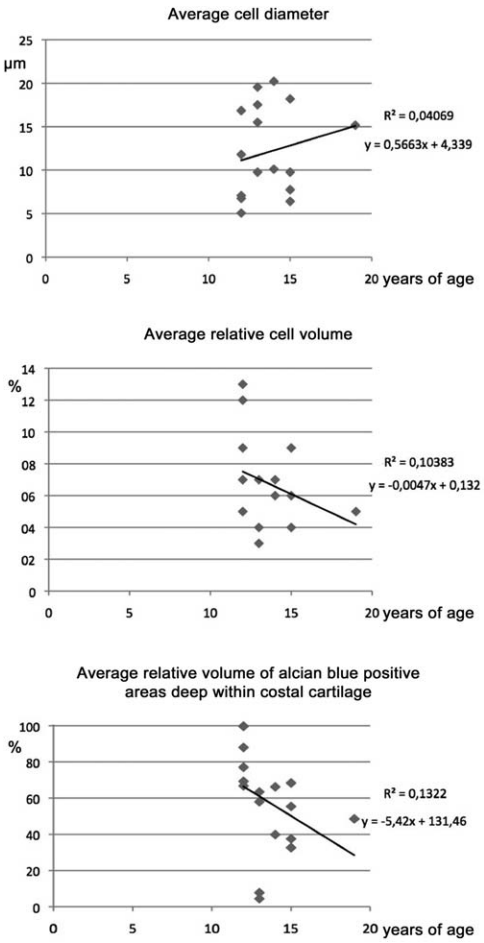

Fig. 2. Correlations between age and morphometrical parameters of cartilage among pectus excavatum patients. No correlation reached significance.

rinsing twice in 1% (w/v) serum albumin in PBS; polyclonal rabbit anti-mouse Ig, biotinylated (Dako, Glostrup, Denmark; #E0464), 1:300 in PBS with 1.5% (w/v) serum albumin, 30 min at room temperature, followed by rinsing twice in PBS; revelation of peroxidase activity with DAB enhanced liquid substrate system (Sigma, #D3939), followed by rinsing twice in distilled water; dehydration and mounting in synthetic medium.

Transmission Electron Microscopy

For electron microscopy, the specimens were osmicated and embedded in epoxy resin. Sections about 1-μm thick were stained with alkaline toluidine blue and used to select the areas for electron microscopic analysis. Sections about 70-nm thick were stained with lead acetate and uranyl acetate and observed in a JEM 1010 electron microscope (Jeol, Tokyo, Japan), at 80 kV.

Statistics

Analysis of variance was used for all comparisons, with significance level set at $P < 0.05$.

RESULTS

In cartilage, chondrocytes appeared mainly isolated or in very small isogenic groups, only exceptionally made by more than three cells. The variable volume fraction occupied by cells depended primarily on cell size rather than on cell number. Chondrocyte size was very heterogeneous in controls and especially large in archive controls of those subjects which were younger than patients. Moreover, cell size, was within the size range of patients in one control within the age range of patients (Fig. 1A,B,D).

Upon alcian blue-safranin staining, the cartilage was alcianophilic near the perichondrium whilst safraninophilic areas were found in several cases in the deeper areas. We found a marked variability among cases in the extent of safraninophilic areas and their distribution (small areas around cells or large inter-territorial areas). Lack of safranin staining was found in four patients, whilst only in two cases alcianophilic areas were restricted to a small portion of tissue. In common with patients, a variable distribution of alcianophilia and safraninophilia was found also in controls (Fig. 1C,E,F).

Quantitative analyses on chondrocytes and extracellular matrix did not show any significant differences between patients and controls. With increasing age, among patients, the cell diameter tended to grow and the relative volume of cells in the tissue and distribution of alcianophilic areas in the matrix tended to decrease, however no correlation reached significance (Table 2; Fig. 2).

Immunohistochemical tagging of collagen type II was seen in cell cytoplasm, in pericellular areas and, to a variable extent, in the interterritorial matrix, in both patients and controls (Fig. 3).

At transmission electron microscopy, in both patients and control cartilage chondrocytes were usually small, poor in organelles, with abundant glycogen and occasional, huge lipid droplets. Only occasionally there were chondrocytes rich in rough endoplasmic reticulum and with extended Golgi apparatus. A thin pericellular zone contained chondrocyte microvilli and little electron-opaque granules corresponding to proteoglycans; a territorial zone hosted thin collagen fibers and proteoglycan granules; and interterritorial zone had thick collagen fibers and less evident proteoglycan granules. A real pericellular capsule was never detected. Small (ca. 100

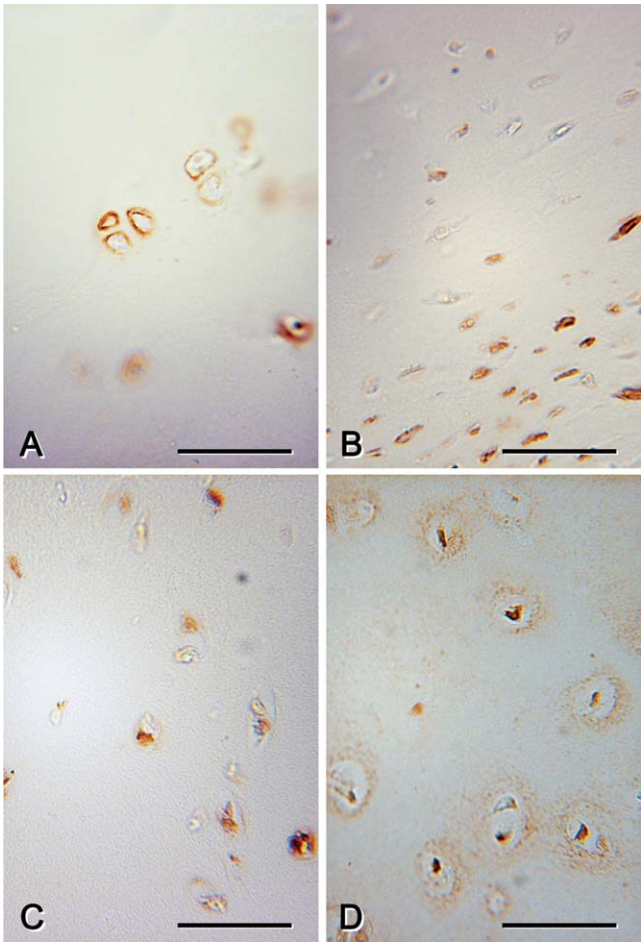

Fig. 3. Collagen type II immunohistochemistry of control and pectus excavatum cartilage. **A–B**: control cartilage. (A) Cartilage from the same subject as Figure 1A: the labeling for type II collagen appears in the cell capsules. (B) Cartilage from the same subject as Figure 1B, immunostained for type II collagen: the labeling appears in the cytoplasm of cells at the periphery of the tissue; the perichondrium was just below the bottom right end of microscopic field. **C–D**: cartilage from pectus excavatum patients. (C) Cartilage of a patient 12-years old: the labeling for type II collagen appears in the cytoplasm. (D) Cartilage of a patient 12-years old: the labeling for type II collagen appears in the cytoplasm and in the extracellular matrix close to cells, corresponding to territorial areas. All panels: anti-Col2 immunoperoxidase without counterstain. Bar = 5 μm.

nm in diameter), membrane bound, round globules with electron dense content were sometimes found in the territorial and in the neighboring interterritorial matrix, with features of so called matrix vesicles Cells were also seen in variable stages of apoptosis, from nuclear and cytoplasmic condensation alternate with vacuoles to blebbing and eventual fragmentation into small electron-opaque vesicles, at all similar to matrix vesicles but collectively delineating the ghost of a cell (Fig. 4). The extracellular matrix intermingled with apoptotic remnants progressively acquired interterritorial features, with many thick collagen fibers and few proteoglycan granules (Fig. 3). Small, occasional fibrillary aggregates were found in just a few cases.

We could not find any correlation between the clinical severity and the cartilage histological features of patients.

DISCUSSION

The main achievement of our study was finding a great variability in the morphologic, morphometric and histochemical features of rib cartilage among a quite high number of patients; these results would have escaped recognition in a smaller sample of cases.

However, upon detailed analysis, we did not discover any specific feature in PE cartilage but rather found signs of cartilage reorganization with time, through cell death and matrix condensation.

The results upon proteoglycan staining have been at variance with those of David et al. (2011), who found most control cartilages to be safraninophilic and the majority (82%) of PE cartilage to be almost exclusively alcianophilic. The patients studied by David et al. (2011) were younger than those analyzed here (age range, 5–18 years vs. 12–20 years), which may explain in part the differences in the results obtained, although within the age range of our patients no correlation between age and histological parameters reached significance. Indeed, our data showed, by increasing age, a tendency to an increase in cell diameter and a decrease in relative volume of cells and in relative volume of alcian blue positive, safranin negative areas.

Surprisingly we found many apoptotic remnants of chondrocytes in our specimen. At the end of the process, they were represented by clusters of small blebs, similar in size and structure to matrix vesicles and delineating the shape, or rather the ghost of a cell. This behavior upon apoptosis may be interpreted as a consequence of the high viscosity of the extracellular matrix and the lack of ameboid movements by chondrocytes, which impairs the approaching of living cells to apoptotic bodies and the phagocytosis of the latter. The small blebs would therefore eventually and progressively dissolve in the matrix, as is supposed for matrix vesicles, which have been proposed to contain enzymes linked to the remodeling of matrix far from cells (Stockwell, 1975). Similar findings have been correlated to chondrocyte apoptosis in thyroid cartilage (Claassen et al., 2009). In the areas of the remnants, collagen fibrils intermingle with the blebs and become more abundant and thick with the decrease in number of the blebs; it may be supposed that the final blebbing represents the conclusion of a process that the cells perform even while perfectly healthy, that is, independently of PE. It is worth noticing that a pericellular capsule was never seen in costal cartilage and that the transition between the pericellular, the territorial and the interterritorial matrix was smooth. The lack of a capsule is at variance with what is known for the chondrocytes of joint cartilage (Stockwell, 1975; Poole et al., 1987). This evidence underscores the difficulty of transferring information from joint cartilage to that elsewhere in the body, where the mechanical load is lower and with different distribution over time.

Occasional alterations of collagen fibrils, such as fibrillary aggregates, were found here as just minor and inconstant findings and therefore should be considered irrelevant to PE pathogenesis.

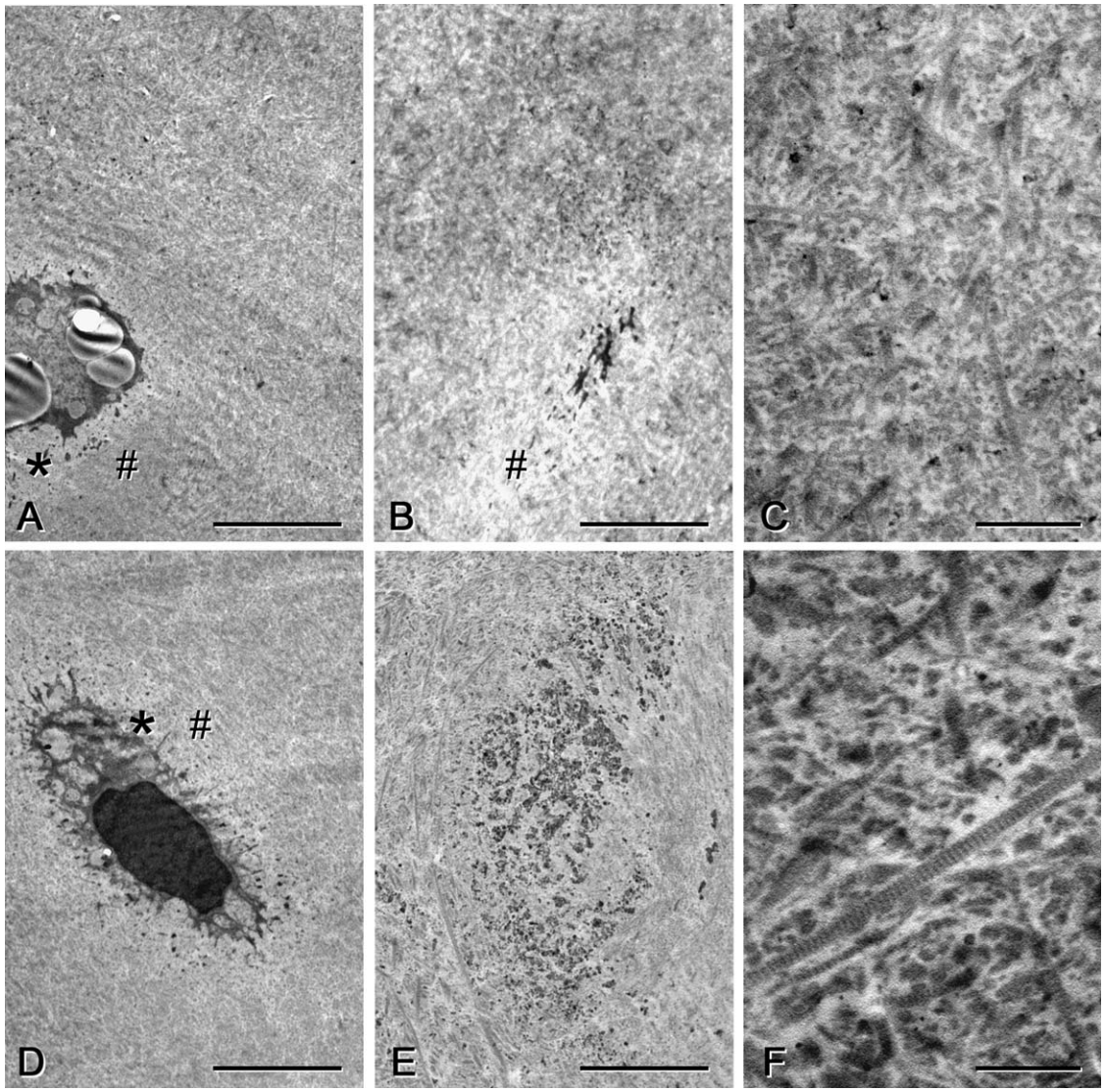

Fig. 4. Electron microscopy of control and pectus excavatum cartilage. **A–C**: control cartilage of an 11-year old control child. **D–E**: cartilage of patients respectively 12 (B) and 13-years old (C, D). Asterisks = pericellular area (cell capsule); # = territorial matrix, characterized by relatively thin, loosely packed collagen fibrils preferentially concentric to cells and surrounded by interterritorial matrix with thicker and densely packed collagen fibrils running in all directions. A, D: viable chondrocytes. B, E: apoptotic remnants of chondrocytes; in advanced cases, marked by marked fragmentation and dispersion of apoptotic bodies (E), the extracellular matrix interspersed with the remnants shows features of interterritorial matrix. Details of interterritorial matrix are given in panels C and F. Bar = 5 μm for panels A, B, D, E and 1 μm for panels C, F.

One strength of our report is that most previous studies on the fine structure and histochemistry of cartilage have focused on joint cartilage. Differently from articular one, costal cartilage is surrounded by a perichondrium—which provides for oxygenation, nutrient and waste exchange and tissue growth—and is not subjected to heavy and quickly variable load. Moreover rib cartilage is not organized into layers depending on the distribution of mechanical load.

The preferred hypothesis for the development of PE has long been primary overgrowth of costal cartilage (Sweet, 1944; Fokin et al., 2009), until Nakaoka et al. (2010) measured costal cartilage length on three-dimensional reconstructions from computerized tomography, in PE patients and control subjects, and found that costal cartilage in PE patients is no longer than in healthy controls.

Of the reports which have investigated the pathogenesis of PE (Rupprecht et al., 1987; Feng et al., 2001; Creswick et al., 2006; Jaroszewski et al., 2010; David et al., 2011), only a few have focused on the structural analysis of rib cartilage, which may be relevant for the pathogenesis of this deformity, and few studies have addressed the histological features of rib cartilage even in control subjects.

Stacey et al. (2012) have shown that both control and PE costal cartilage is characterized by small isogenic

groups (ca. 90% cells were single or in doublets) and that centrally located cells produce higher amounts of aggrecan than peripheral cells.

Feng et al. (2001) have also found similar staining properties by safranin between control and PE cartilage, with a tendency to heavier staining of the deep than the superficial areas, nor did they find relevant differences in cell structure between control and PE cartilage at light and electron microscopy; upon this latter analysis, they described a more irregular distribution of collagen fibrils in the deep areas of PE than of control cartilage, which was not confirmed by the present study.

In early stages of our research on PE, we analyzed also rib bone and skin specimens in order to check for possibly relevant histopathological features. Before undergoing minimally invasive surgical procedure under thoracoscopic guidance, every patient underwent a thorough clinical check and we were unable to find any kind of correlation between histopathological and clinical features, nor found hints in that direction in the literature. Moreover, rib cartilage was evaluated by means of preoperative chest nuclear magnetic resonance: we were not able to find any difference in terms of breadth and length, when compared with healthy controls from the same age group, as reported in previous descriptions (Nakaoka et al., 2010).

The present results implement and in part confirm the studies mentioned above, inasmuch they demonstrate the peculiarities of costal cartilage as compared with the articular cartilage (Stockwell, 1975; Poole et al., 1987) and do not show peculiarities for PE which may be possibly explicative of its pathogenesis.

Our findings rather suggest that the costal cartilage undergoes a morphological stabilization with time through a decrease in cell density and condensation of the collagen meshwork, thus making its shape definitive whether normal or dysmorphic.

In conclusion, since neither morphology at different levels of analysis nor biochemistry have yet succeeded to identify specific features of PE costal cartilage, it seems reasonable to propose—for the moment being—that only dynamic forces are at work leading to chest deformation and that cartilage metabolism just fixes the shape that has been achieved.

ACKNOWLEDGEMENTS

The authors are grateful to Dr. Giulio Ravoni (Department of Pediatric Surgery, Children's Hospital A. Meyer, Florence, Italy) for his precious help with data collection.

LITERATURE CITED

Bardakhch'ian EA, Chepurnoĭ GI, Shamik VB. 2002. Ultrastructural changes of child rib cartilage in different deformations of chest cells. Arkh Patol 64:40–45.

Brochhausen C, Turial S, Muller FK, Schmitt VH, Coerdt W, Wihlm JM, Schier F, Kirkpatrick CJ. 2012. Pectus excavatum: history, hypotheses and treatment options. Interact Cardiovasc Thorac Surg 14:801–806.

Cartoski MJ, Nuss D, Goretsky MJ, Proud VK, Croitoru DP, Gustin T, Mitchell K, Vasser E, Kelly RE, Jr. 2006. Classification of the dysmorphology of pectus excavatum. J Pediatr Surg 41:1573–1581.

Chaffins JA. 2007. Marfan syndrome. Radiol Technol 78:222–236; quiz 237–229.

Claassen H, Schicht M, Sel S, Werner J, Paulsen F. 2009. The fate of chondrocytes during ageing of human thyroid cartilage. Histochem Cell Biol 131:605–614.

Creswick HA, Stacey MW, Kelly RE, Jr, Gustin T, Nuss D, Harvey H, Goretsky MJ, Vasser E, Welch JC, Mitchell K, Proud VK. 2006. Family study of the inheritance of pectus excavatum. J Pediatr Surg 41:1699–1703.

David VL, Izvernariu DA, Popoiu CM, Puiu M, Boia ES. 2011. Morphologic, morphometrical and histochemical proprieties of the costal cartilage in children with pectus excavatum. Rom J Morphol Embryol 52:625–629.

Dietz HC. 1992. Molecular biology of Marfan syndrome. J Vasc Surg 15:927–928.

Feng J, Hu T, Liu W, Zhang S, Tang Y, Chen R, Jiang X, Wei F. 2001. The biomechanical, morphologic, and histochemical properties of the costal cartilages in children with pectus excavatum. J Pediatr Surg 36:1770–1776.

Fenton JE, Fagan PA. 1996. Meatoplasty in Marfan syndrome. J Laryngol Otol 110:456–458.

Fokin AA, Steuerwald NM, Ahrens WA, Allen KE. 2009. Anatomical, histologic, and genetic characteristics of congenital chest wall deformities. Semin Thorac Cardiovasc Surg 21:44–57.

Glesby MJ, Pyeritz RE. 1989. Association of mitral valve prolapse and systemic abnormalities of connective tissue. A phenotypic continuum. JAMA 262:523–528.

Golladay ES, Char F, Mollitt DL. 1985. Children with Marfan's syndrome and pectus excavatum. South Med J 78:1319–1323.

Jaroszewski D, Notrica D, McMahon L, Steidley DE, Deschamps C. 2010. Current management of pectus excavatum: a review and update of therapy and treatment recommendations. J Am Board Fam Med 23:230–239.

Judge DP, Dietz HC. 2005. Marfan's syndrome. Lancet 366:1965–1976.

Le Parc JM, Molcard S, Tubach F, Boileau C, Jondeau G, Muti C, Chevallier B, Pisella PJ. 2000. Marfan syndrome and fibrillin disorders. Joint Bone Spine 67:401–407.

Loeys BL, Dietz HC, Braverman AC, Callewaert BL, De Backer J, Devereux RB, Hilhorst-Hofstee Y, Jondeau G, Faivre L, Milewicz DM, Pyeritz RE, Sponseller PD, Wordsworth P, De Paepe AM. 2010. The revised Ghent nosology for the Marfan syndrome. J Med Genet 47:476–485.

Mortensen K, Baulmann J, Rybczynski M, Sheikhzadeh S, Aydin MA, Treede H, Dombrowski E, Kuhne K, Peitsmeier P, Habermann CR, Robinson PN, Stuhrmann M, Berger J, Meinertz T, von Kodolitsch Y. 2010. Augmentation index and the evolution of aortic disease in marfan-like syndromes. Am J Hypertens 23: 716–724.

Nakaoka T, Uemura S, Yoshida T, Tanimoto T, Miyake H. 2010. Overgrowth of costal cartilage is not the etiology of pectus excavatum. J Pediatr Surg 45:2015–2018.

Nogami H, Oohira A, Ozeki K, Oki T, Ogino T, Murachi S. 1979. Ultrastructure of cartilage in heritable disorders of connective tissue. Clin Orthop Relat Res 143:251–259.

Nollen GJ, Mulder BJ. 2004. What is new in the Marfan syndrome? Int J Cardiol 97 (Suppl 1):103–108.

Nuss D, Kelly RE, Jr, Croitoru DP, Katz ME. 1998 A 10-year review of a minimally invasive technique for the correction of pectus excavatum. J Pediatr Surg 33:545–552.

Olbrecht VA, Nabaweesi R, Arnold MA, Chandler N, Chang DC, McIltrot KH, Abdullah F, Paidas CN, Colombani PM. 2009. Pectus bar repair of pectus excavatum in patients with connective tissue disease. J Pediatr Surg 44:1812–1816.

Poole AR, Witter J, Roberts N, Roughley PJ, Webber C, Campbell I. 1987. Immunodetection and characterization of the degradation of cartilage proteoglycans in vitro and in vivo. J Rheumatol 14:80–82.

Redlinger RE, Jr, Rushing GD, Moskowitz AD, Kelly RE, Jr, Nuss D, Kuhn A, Obermeyer RJ, Goretsky MJ. 2010. Minimally invasive repair of pectus excavatum in patients with Marfan syndrome and marfanoid features. J Pediatr Surg 45:193–199.

Rupprecht H, Hummer HP, Stoss H, Waldherr T. 1987. Pathogenesis of chest wall abnormalities—Electron microscopy studies and trace element analysis of rib cartilage. Z Kinderchir 42:228–229.

Scherer LR, Arn PH, Dressel DA, Pyeritz RM, Haller JA, Jr. 1988. Surgical management of children and young adults with Marfan syndrome and pectus excavatum. J Pediatr Surg 23:1169–1172.

Shimode N, Itani M, Yada S, Arimura Y, Tsujimoto S, Tashiro C. 2007. Unexpected tracheobronchomalacia during cardiac operation in a patient with Marfan's syndrome. Masui 56:414–417.

Stacey MW, Grubbs J, Asmar A, Pryor J, Elsayed-Ali H, Cao W, Beskok A, Dutta D, Darby DA, Fecteau A, Werner A, Kelly RE, Jr. 2012. Decorin expression, straw-like structure, and differentiation of human costal cartilage. Connect Tissue Res 53:415–421.

Stockwell RA. 1975. Structural and histochemical aspects of the pericellular environment in cartilage. Philos Trans R Soc Lond B Biol Sci 271:243–245.

Stuart AG, Williams A. 2007. Marfan's syndrome and the heart. Arch Dis Child 92:351–356.

Sweet RH. 1944. Pectus excavatum: Report of two cases successfully operated upon. Ann Surg 119:922–934.

Tocchioni F, Ghionzoli M, Pepe G, Messineo A. 2012. Pectus excavatum and MASS phenotype: an unknown association. J Laparoendosc Adv Surg Tech A 22:5.

Van de Velde S, Fillman R, Yandow S. 2005. Protrusio acetabuli in Marfan syndrome: indication for surgery in skeletally immature Marfan patients. J Pediatr Orthop 25:603–606.